ISBN: 978-3-95450-184-7 doi:10.18429/JACoW-IPAC2018-THPMK058

RF DESIGN OF THE X-BAND LINAC FOR THE EUPRAXIA@SPARC_LAB PROJECT

M. Diomede*[1], D. Alesini, M. Bellaveglia, B. Buonomo, F. Cardelli, E. Chiadroni, G. Di Raddo, R. Di Raddo, M. Ferrario, A. Gallo, A. Ghigo, A. Giribono, V. Lollo, L. Piersanti, B. Spataro, C. Vaccarezza, INFN-LNF, Via E. Fermi 40, Frascati, Italy
N. Catalan Lasheras, A. Grudiev, W. Wuensch, CERN, CH-1211 Geneva-23, Switzerland
[1]also at Sapienza University, Piazzale Aldo Moro 5, Roma, Italy

Abstract

We illustrate the RF design of the X-band linac for the upgrade of the SPARC_LAB facility at INFN-LNF (EuPRAXIA@SPARC_LAB). The structures are traveling wave (TW) cavities, working on the $2\pi/3$ mode, fed by klystrons with pulse compressor systems. The tapering of the cells along the structure and the cell profiles have been optimized to maximize the effective shunt impedance keeping under control the maximum value of the modified Poynting vector, while the couplers have been designed to have a symmetric feeding and a reduced pulsed heating. In the paper we also present the RF power distribution layout of the accelerating module and a preliminary mechanical design.

INTRODUCTION

EuPRAXIA@SPARC_LAB [1] is the foreseen upgrade of the SPARC_LAB test facility at INFN-LNF (Frascati, Italy) [2]. It might be one of the possible candidates to host EuPRAXIA (European Plasma Research Accelerator with eXcellence In Applications) [3]. The purpose of the project is to bring together, for the first time, novel acceleration schemes, modern lasers, the latest correction/feedback technologies and large-scale user areas.

The preliminary EuPRAXIA@SPARC_LAB linac layout is based on an S-band Gun, three S-band TW structures and an X-band booster with a bunch compressor. The X-band technology allows to reach a high accelerating gradient and a high facility compactness, which are some of the goals of the projects. The accelerating structures are TW cavities fed by klystrons and pulse compressor systems. The operating mode is the $2\pi/3$ mode at the frequency of 11.9942 GHz.

Two different scenarios are foreseen: acceleration with and without plasma stage. In the second case (named full RF), two average gradients are foreseen: 57 MV/m (high-gradient case, HG) and 80 MV/m (very high-gradient case, VHG). The second value has been considered for the booster design and optimization.

In this paper we illustrate the electromagnetic (e.m.) design of the single cell, the numerical optimization of the X-band booster and the preliminary results of the input coupler design. In the second part, the preliminary mechanical design of the single cell and layout of the accelerating module are shown.

* marco.diomede@lnf.infn.it

ELECTROMAGNETIC DESIGN

The X-band booster design has been performed following two main steps: e.m. design of the single cell and numerical optimization of the booster on the basis of the single cell results. The input coupler has then been designed. The designs of single cell and coupler have been performed using the 3D e.m. code ANSYS Electronics Desktop [4].

Cell Design

The design aimed to minimize the modified Poynting vector normalized to the average accelerating gradient S_{cmax}/E^2_{acc} [5] and to calculate the other cell parameters (shunt impedance per unit length R, quality factor Q and the group velocity v_g/c) as a function of the iris aperture a. A sketch of the cell is shown in Fig. 1. According to beam dynamics simulations and beam break-up limits [6], an average iris radius of 3.2 mm has been chosen.

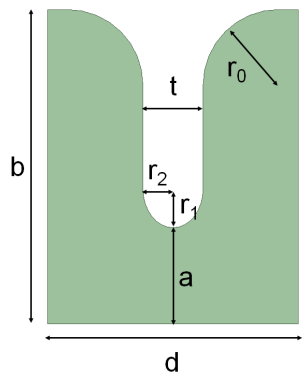

Figure 1: Sketch of the single cell with main parametrized dimensions.

An elliptical shape of the irises has been considered and the modified Poynting vector as a function of the iris ellipticity r_1/r_2 has been calculated (Fig. 2). The minimum value of S_{cmax}/E^2_{acc} has been obtained for $r_1/r_2 = 1.3$. The cell parameters are summarized in Table 1. The other mentioned cell parameters, as a function of the iris radius a, have then been calculated (Fig. 3).

Structure Design

The analytical formulas of TW structure [7] and SLED pulse compressor [8] have been implemented in a numerical tool able to calculate the main structure parameters for a

ISBN: 978-3-95450-184-7 doi:10.18429/JACoW-IPAC2018-THPMK058

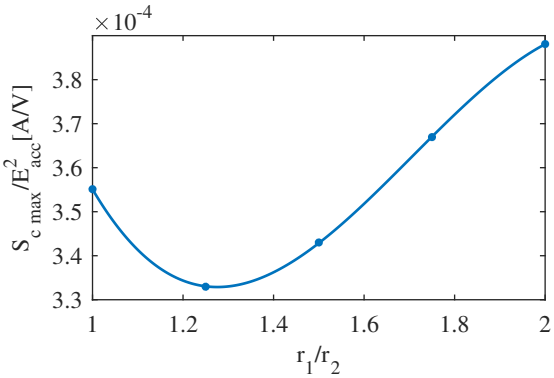

Figure 2: Modified Poynting vector as a function of the iris ellipticity (a = 3.2 mm).

Table 1: Single Cell Parameters for a = 3.2 mm

Iris radius a [mm]	3.2
Iris thickness t [mm]	2.0
Iris ellipticity r_1/r_2	1.3
Edge rounding radius r_0 [mm]	2.5
Outer radius b [mm]	10.452
Cell length d [mm]	8.332
R [MΩ/m]	117
v_g/c [%]	1.77
Q	7036
$S_{c\,max}/E^2_{acc}$ [A/V]	$3.3 \cdot 10^{-4}$

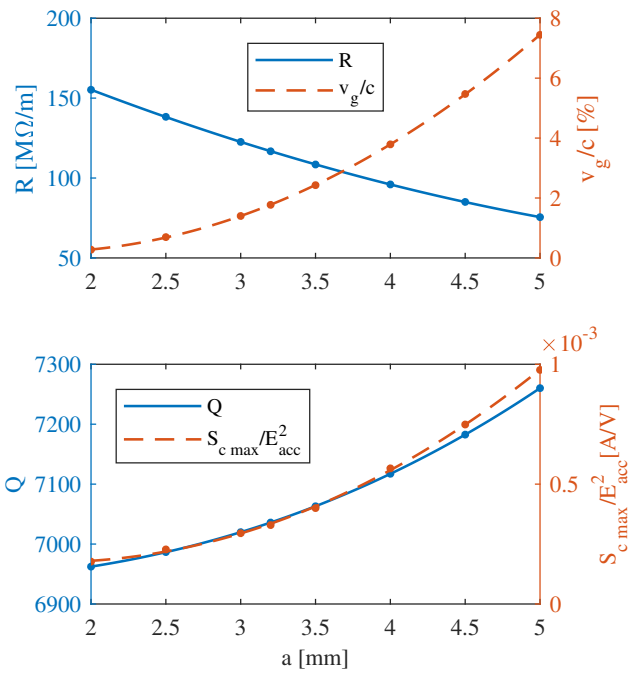

Figure 3: Single cell parameters as a function of the iris radius.

given structure length and an arbitrary cell-by-cell iris modulation along the structure itself [9]. In particular, we have considered linear iris tapered structures as sketched in Fig. 4.

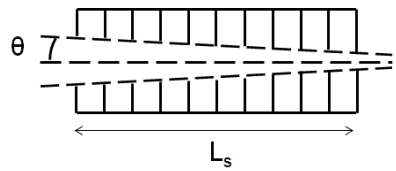

Figure 4: Sketch of the cell-by-cell iris tapering.

The effective shunt impedance R_s of the structure [10] and the peak value of the modified Poynting vector have been calculated as a function of the iris tapering angle θ for different structure lengths. As an example, in Fig. 5 we report R_s for three different lengths, while in Fig. 6 it is shown $S_{c\,max}/E^2_{acc}$ of L_s = 0.5 m and for an average accelerating field equal to 80 MV/m. In the same plot, we have also reported the theoretical value that, according to [11], corresponds to a breakdown rate (BDR) of 10^{-6} bpp/m.

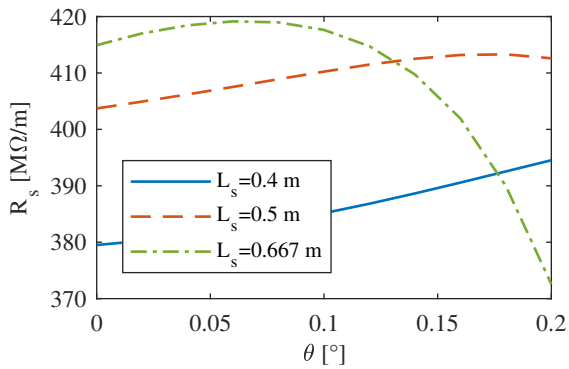

Figure 5: Effective shunt impedance as a function of the iris tapering angle for three different structure lengths.

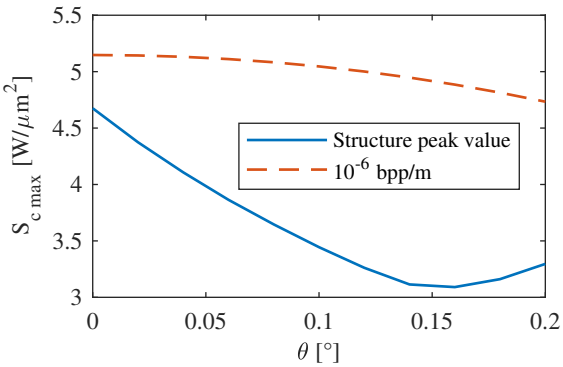

Figure 6: Peak value of modified Poynting vector as a function of the iris tapering angle for L_s = 0.5 m (VHG case).

As a reference design of the structure, we have finally considered 0.5 m long structures with a tapering angle of 0.1° as a good compromise between modularity, R_s and iris tapering. In fact, this gives a total number of structures equal to 32 that can be easily divided into groups of 8 structures fed by 1 klystron in the HG case and 2 klystrons in parallel in the

ISBN: 978-3-95450-184-7 doi:10.18429/JACoW-IPAC2018-THPMK058

VHG case. In both cases the RF pulse will be compressed by means of 1 SLED [9]. The X-band linac main parameters are shown in Table 2.

Table 2: X-band Linac Parameters

Frequency of operation [GHz]	11.9942	
Peak klystron power [MW]	50	
Available klystron power [MW]	≈ 40	
Klystron pulse length t_k [μs]	1.5	
Structure filling time t_f [ns]	100	
Unloaded Q-factor Q_0 of SLED	180000	
External Q-factor Q_e of SLED	19300	
a first-last cell [mm]	3.636 – 2.764	
v_g/c first-last cell [%]	2.77 – 1.02	
R_s [MΩ/m]	410	
Structure length L_s [m]	0.5	
Booster active length L_t [m]	16	
No. of structures N_s	32	
Average gradient $\langle G \rangle$ [MV/m]	57	80
Energy gain W_{gain} [MeV]	912	1280
Total required RF power P_{RF} [MW]	127	250
No. of klystrons N_k	4	8
Input coupler pulsed heating [°C]		<26

Input Coupler Preliminary Design

As a first case, we have considered a z-type coupler because of its compactness with respect to the waveguide and mode-launcher types. We have calculated, in particular, the pulsed heating [12, 13] in the VHG case. In Fig. 7, the geometry of the coupler and the surface magnetic field are reported. We have considered a dual feeding in order to cancel the dipole field components introduced by the coupling holes. The calculated pulsed heating on the input coupler is <26 °C, while the obtained reflection coefficient is <−30 dB. Racetrack geometries will be considered in order to compensate for the residual quadrupole field components.

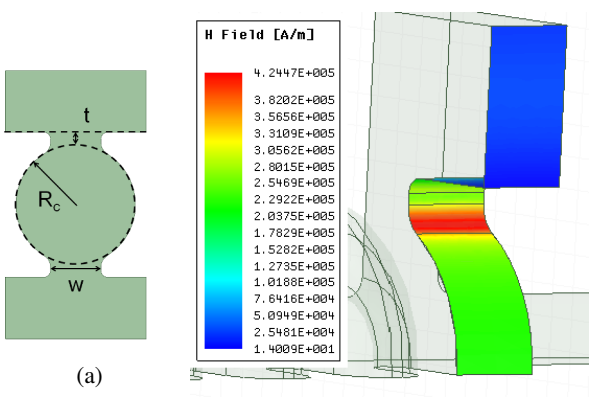

(a) (b)

Figure 7: Sketch of the front view of the input coupler (a), surface magnetic field distribution of the input coupler (b).

PRELIMINARY MECHANICAL DESIGN AND RF MODULE LAYOUT

A mechanical design activity has been started. The mechanical 3D model of the single cell is given in Fig. 8. The cells will integrate four symmetric cooling channels. By means of a prototype activity, we are exploring the possibility to avoid the tuning of the cells.

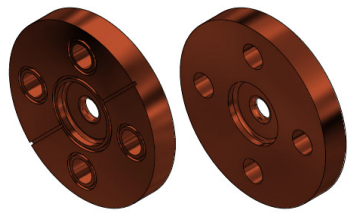

Figure 8: Mechanical drawings of the single cell.

The preliminary layout of the RF module with the power distribution waveguide network is shown in Fig. 9 in the HG case. A low-loss circular waveguide will connect the RF power sources (in klystron gallery) to the accelerating module (in the experimental hall). Downstream the circular waveguide, the SLED will compress the RF pulses while a system of seven 3 dB hybrid splitter will distribute the RF power to the 8 structures of the module itself. The module will also integrate the vacuum pumping system, the magnets and the diagnostics. Calculations on the final waveguide distribution attenuation and vacuum pressures are still in progress.

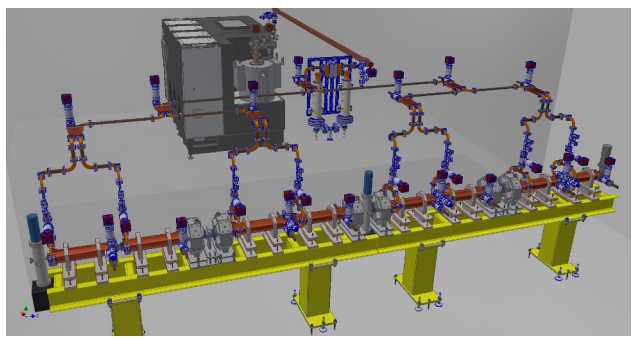

Figure 9: Layout of a single accelerating module.

CONCLUSION

In this paper we have illustrated the preliminary RF design of the EuPRAXIA@SPARC_LAB X-band linac. The single cell geometry has been optimized by e.m. simulations, minimizing the modified Poynting vector normalized to the average accelerating field. A numerical optimization of the whole structure has been performed (maximization of the RF efficiency and minimization of the expected BDR). A preliminary e.m. design of the input coupler has also been performed. Finally, a preliminary mechanical design of the cell and the layout of the RF module have been presented.

ISBN: 978-3-95450-184-7 doi:10.18429/JACoW-IPAC2018-THPMK058

REFERENCES

[1] M. Ferrario *et al.*, "EuPRAXIA@SPARC_LAB Design study towards a compact FEL facility at LNF," *Nucl. Instrum. Meth. A*, 2018, in press. DOI: https://doi.org/10.1016/j.nima.2018.01.094

[2] M. Ferrario *et al.*, "SPARC_LAB present and future," *Nucl. Instrum. Meth. B*, vol. 309, pp. 183–188, 2013.

[3] P. Walker *et al.*, "HORIZON 2020 EuPRAXIA Design Study," in *Proc. of IPAC2017, TUOBB3, Copenhagen, Denmark*, 2017.

[4] *ANSYS Electronics Desktop website*, http://www.ansys.com/products/electronics/ansys-electronics-desktop

[5] A. Grudiev, S. Calatroni, and W. Wuensch, "New local field quantity describing the high gradient limit of accelerating structures," *Physical Review Special Topics-Accelerators and Beams*, vol. 12, p. 102 001, 2009.

[6] C. Vaccarezza *et al.*, "EUPRAXIA@SPARC_LAB: Beam dynamics studies for the X-band Linac," *Nucl. Instrum. Meth. A*, 2018, in press. DOI: https://doi.org/10.1016/j.nima.2018.01.100

[7] A. Lunin, V. Yakovlev, and A. Grudiev, "Analytical solutions for transient and steady state beam loading in arbitrary traveling wave accelerating structures," *Phys. Rev. ST Accel. Beams*, vol. 14, p. 052 001, 5 May 2011.

[8] Z. Farkas, H. Hogg, G. Loew, and P. Wilson, "SLED: A method of doubling SLAC's energy," in *Proc. of 9th Int. Conf. on High Energy Accelerators, SLAC*, 1974, p. 576.

[9] M. Diomede *et al.*, "Preliminary RF design of an X-band linac for the EuPRAXIA@SPARC_LAB project," *Nucl. Instrum. Meth. A*, 2018, in press. DOI: https://doi.org/10.1016/j.nima.2018.01.032

[10] R. B. Neal, "Design of Linear Electron Accelerators with Beam Loading," *Journal of Applied Physics*, vol. 29, no. 7, pp. 1019–1024, 1958.

[11] K. Sjobak, E. Adli, and A. Grudiev, "New Criterion for Shape Optimization of Normal-Conducting Accelerator Cells for High-Gradient Applications," in *Proc. of LINAC2014, MOPP028, Geneva, Switzerland*, 2014.

[12] D. Pritzkau, "RF pulsed heating," PhD thesis, 2001.

[13] V. Dolgashev, "High magnetic fields in couplers of X-band accelerating structures," in *Proceedings of the 2003 Particle Accelerator Conference*, IEEE, vol. 2, 2003, pp. 1267–1269.